

Eulerian-Lagrangian discontinuous Galerkin method for transport problems and its application to nonlinear Vlasov dynamics

Jing-Mei Qiu

Department of Mathematical Sciences
University of Delaware

Joint work with S. Boscarino, X. Cai, W. Guo, and Y. Yang

Advances and Challenges in Hyperbolic Conservation Laws, ICERM, May. 2021.

Outline

Semi-Lagrangian discontinuous Galerkin method

- SLDG algorithm

- Numerical results

Eulerian-Lagrangian RK discontinuous Galerkin method

- ELDG algorithm

- Numerical results

Runge-Kutta Exponential Integrators

- SLDG/ELDG-RKEI methods

- Nonlinear model: the guiding center Vlasov model

Conclusions

SL schemes

SLDG method:

- ▶ DG: Low numerical dissipation; compactness; flexibility for boundary and parallel implementation; superconvergence.
- ▶ SL: Could take **extra large time stepping size** with accuracy and stability, leading to gain in efficiency.
- ▶ Backward SL: **Mass conservation** can be preserved.

Applications

- ▶ Plasma application: Vlasov equation.
- ▶ Climate modeling
- ▶ Fluid and kinetic models.

1D SLDG for the linear transport equation*

Consider a 1D linear transport problem

$$\frac{\partial u}{\partial t} + \frac{\partial}{\partial x}(a(x, t)u) = 0$$

with appropriate initial and boundary conditions.

We consider **an adjoint problem for the test function** $\psi(x, t)$:

$$\begin{cases} \psi_t + a(x, t)\psi_x = 0, \\ \psi(t = t^{n+1}) = \Psi(x), \end{cases}$$

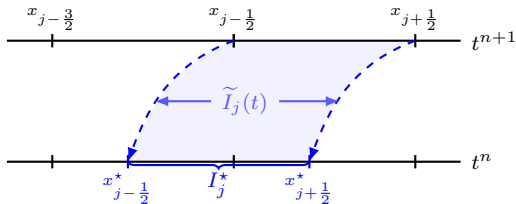
which is in an advective form, hence ψ stays constant along the characteristics.

*Cai-Guo-Q., JSC, 2017

It can be shown that

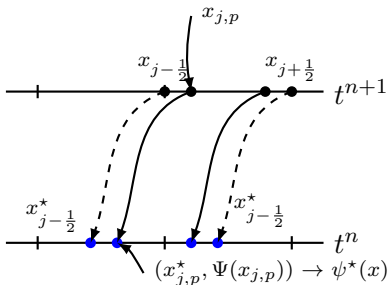
$$\frac{d}{dt} \int_{\tilde{I}_j(t)} u(x, t) \psi(x, t) dx = 0, \quad (1)$$

where $\tilde{I}_j(t)$ is a dynamic interval bounded by characteristics emanating from cell boundaries of I_j at $t = t^{n+1}$.



Thus, from equation (1),

$$\int_{I_j} u(x, t^{n+1}) \Psi(x, t^{n+1}) dx = \int_{I_j^*} u(x, t^n) \psi(x, t^n) dx.$$



Two dimensional SLDG[‡]

- ▶ Consider a two-dimensional linear transport problem

$$\frac{\partial u}{\partial t} + \frac{\partial}{\partial x}(a(x, y, t)u) + \frac{\partial}{\partial y}(b(x, y, t)u) = 0$$

with appropriate initial and boundary conditions.

- ▶ Weak formulation of characteristic Galerkin method[†]: an adjoint problem for the test function $\psi(x, y, t)$

$$\begin{cases} \psi_t + a(x, y, t)\psi_x + b(x, y, t)\psi_y = 0, \\ \psi(t = t^{n+1}) = \Psi(x, y). \end{cases}$$

Then it can be shown that $\forall \psi \in P^k(A_j)$,

$$\frac{d}{dt} \int_{\tilde{A}_j(t)} u(x, y, t)\psi(x, y, t) dx dy = 0$$

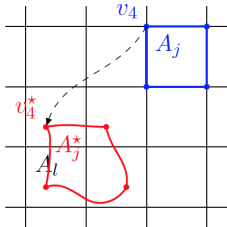
with $\tilde{A}_j(t)$ a dynamic interval bounded by characteristics emanating from cell boundaries of A_j at $t = t^{n+1}$.

[†]Guo, Nair and Q., MWR, 2014.

[‡]Cai, Guo and Q., JSC, 2017.

$$\int_{A_j} u(x, y, t^{n+1}) \Psi(x, y) dx dy = \int_{A_j^*} u(x, y, t^n) \psi(x, y, t^n) dx dy$$

with A_j and A_j^* are shown as in the below left plot.

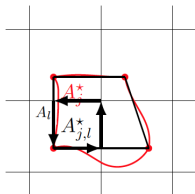
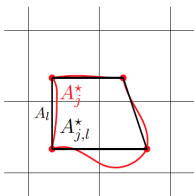


- Characteristics tracing: Locate four vertices of upstream cell A_j^* : v_q^* ($q = 1, 2, 3, 4$) by solving the characteristics equations,

$$\begin{cases} \frac{dx(t)}{dt} = a(x(t), y(t), t), \\ \frac{dy(t)}{dt} = b(x(t), y(t), t), \\ x(t^{n+1}) = x(v_q), \\ y(t^{n+1}) = y(v_q), \end{cases}$$

starting from the four vertices of A_j : v_q ($q = 1, 2, 3, 4$).

Evaluation of $\int_{A_j^*} u(x, y, t^n) \psi(x, y, t^n) dx dy$



Two observations:

- ▶ $\psi(x, y, t^n)$ may not be a polynomial.
- ▶ $u(x, y, t^n)$ is a piecewise polynomial function on background cells.

Strategies:

- ▶ Reconstruct $\psi^*(x, y)$ approximating $\psi(x, y, t^n)$ on A_j^* by a least square strategy, based on

$$\psi(x(v_q^*), y(v_q^*), t^n) = \Psi(x(v_q), y(v_q)),$$

$$q = 1, 2, 3, 4.$$

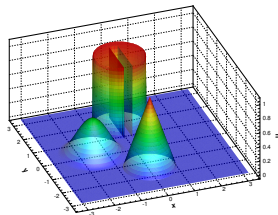
- ▶ Evaluation of the integrand over the upstream cell has to be done subregion-by-subregion.

The swirling deformation problem.

$$u_t - \left(\cos^2\left(\frac{x}{2}\right) \sin(y) g(t) u \right)_x + \left(\sin(x) \cos^2\left(\frac{y}{2}\right) g(t) u \right)_y = 0,$$

with

- ▶ $g(t) = \cos\left(\frac{\pi t}{T}\right) \pi$,
- ▶ $x \in [-\pi, \pi]$, $y \in [-\pi, \pi]$,
- ▶ The initial condition as shown on the right.



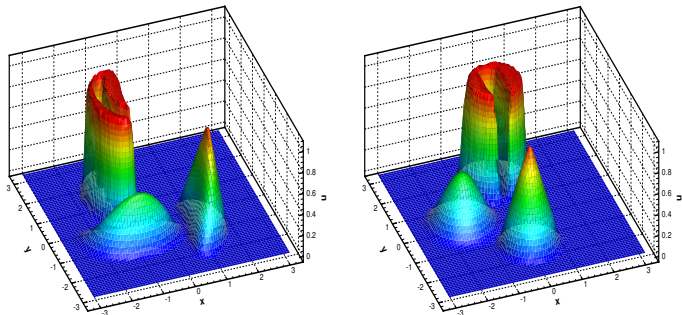


Figure: Swirling deformation problem. Third order SL DG scheme: $T = 0.75$ (left) and $T = 1.5$ (right). The numerical mesh is 80×80 with $CFL = 5$.

The swirling deformation problem: convergence study

Table:

$u_t - \left(\cos^2\left(\frac{x}{2}\right) \sin(y) \cos\left(\frac{2\pi t}{3}\right) \pi u\right)_x + \left(\sin(x) \cos^2\left(\frac{y}{2}\right) \cos\left(\frac{2\pi t}{3}\right) \pi u\right)_y = 0$. The initial condition is a smooth cosine bell. $T = 1.5$.

Mesh	L^2 error	Order	L^2 error	Order
P^1 SLDG	CFL = π		CFL = 5π	
20×20	1.25E-02		8.59E-03	
40×40	2.92E-03	2.10	2.14E-03	2.00
80×80	5.96E-04	2.29	5.42E-04	1.98
160×160	1.30E-04	2.20	1.33E-04	2.02
P^2 SLDG				
20×20	3.22E-03		9.37E-03	
40×40	6.58E-04	2.29	2.87E-03	1.71
80×80	1.42E-04	2.22	6.92E-04	2.05
160×160	3.15E-05	2.17	1.89E-04	1.87
P^2 SLDG-QC				
20×20	2.61E-03		5.29E-03	
40×40	3.15E-04	3.05	7.78E-04	2.77
80×80	3.81E-05	3.05	1.04E-04	2.90
160×160	4.91E-06	2.96	1.47E-05	2.83

Properties of the scheme

Convection equations in a conservative form

$$u_t + \nabla_{\mathbf{x}} \cdot (\mathbf{a}u) = 0.$$

A SLDG discretization of

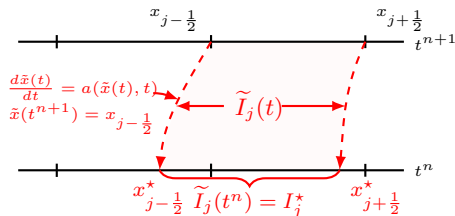
$$u^{n+1} = SLDG(\mathbf{a}, \Delta t)u^n.$$

- ▶ Mass conservation.
- ▶ High order accuracy in space and time.
- ▶ Unconditionally stability which allows arbitrary large stepping size.
- ▶ No dimensional splitting error for multi-dimensional problems.

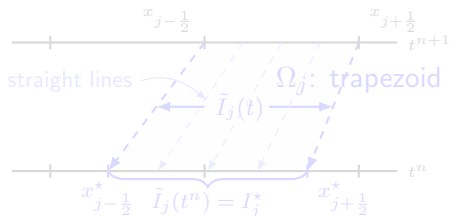
Motivation of ELDG

- ▶ Motivation
 - ▶ Higher dimensional problem: complication from quadratic curve approximations to sides of upstream cells.
 - ▶ General nonlinear problems: characteristics tracing is difficult or impossible.
- ▶ Related work in literature
 - ▶ Eulerian-Lagrangian localized adjoint methods (ELLAM): Douglas and Russel (82'), Celia, Ewing, Wang, etc.
 - ▶ Eulerian-Lagrangian WENO method: Huang, Arbogast, et. al. 2016
 - ▶ Arbitrary Lagrangian-Eulerian (ALE) moving mesh method.

The space-time region of ELDG

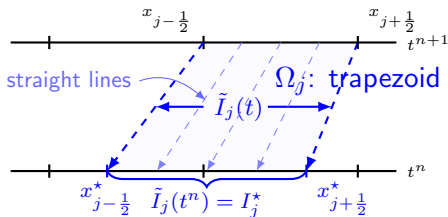
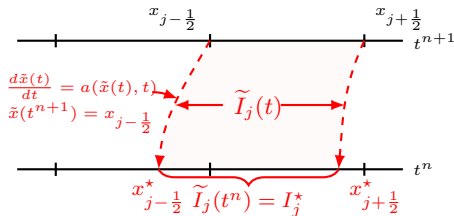


$$\frac{d}{dt} \int_{\tilde{I}_j(t)} u(x, t) \psi(x, t) dx = 0.$$



- ▶ Linear function $\alpha(x, t)$ in approximating $a(x, t)$.
- ▶ Feature I: Ω_j : trapezoid; in high-D upstream cells are polygons (tetrahedron).
- ▶ Feature II: straight lines approximating characteristics.

The space-time region of ELDG



$$\frac{d}{dt} \int_{\tilde{I}_j(t)} u(x, t) \psi(x, t) dx = 0.$$

- ▶ Linear function $\alpha(x, t)$ in approximating $a(x, t)$.
- ▶ Feature I: Ω_j : trapezoid; in high-D upstream cells are polygons (tetrahedron).
- ▶ Feature II: straight lines approximating characteristics.

ELDG for 1D linear transport: A modified adjoint problem

- ▶ We consider

$$u_t + (a(x, t)u)_x = 0. \quad (2)$$

- ▶ We consider the adjoint problem with $\forall \Psi \in P^k(I_j)$ on the time interval $[t^n, t^{n+1}]$:

$$\begin{cases} \psi_t + \alpha(x, t)\psi_x = 0, & t \in [t^n, t^{n+1}], \\ \psi(t = t^{n+1}) = \Psi(x), \end{cases} \quad (3)$$

with $\alpha(x, t)$ being a linear approximation to the original velocity field $a(x, t)$.

The semi-discrete ELDG scheme

$$\int_{\Omega_j} [(2) \cdot \psi + (3) \cdot u] dx dt = 0.$$

It leads to

$$\boxed{\frac{d}{dt} \int_{\tilde{I}_j(t)} (u\psi) dx = - (F\psi) \Big|_{\tilde{x}_{j+\frac{1}{2}}(t)} + (F\psi) \Big|_{\tilde{x}_{j-\frac{1}{2}}(t)} + \int_{\tilde{I}_j(t)} F\psi_x dx.} \quad (4)$$

where $F(u) \doteq (a - \alpha)u$.

- ▶ In special case of $\alpha(x, t) = 0$, ELDG becomes RKDG;
- ▶ In special case of $\alpha(x, t) = a(x, t)$, ELDG becomes SLDG.

The semi-discrete ELDG scheme (cont.)

$$\frac{d}{dt} \int_{I_j} (u \Psi(\xi)) \frac{\partial \tilde{x}(t; (\xi, t^{n+1}))}{\partial \xi} d\xi = - (\hat{F} \Psi) \Big|_{\xi=x_{j+\frac{1}{2}}} + (\hat{F} \Psi) \Big|_{\xi=x_{j-\frac{1}{2}}} + \int_{I_j} F \Psi_{\xi} d\xi.$$

- ▶ Lax-Friedrich flux:

$$\hat{F}(u^-, u^+) = \frac{1}{2}(F(u^-) + F(u^+)) + \frac{\alpha_0}{2}(u^- - u^+), \alpha_0 = \max_u |F'(u)|.$$

- ▶ $k + 1$ points Gauss quadrature rules :

$$\int_{I_j} F(u_h) \Psi_{\xi} d\xi \approx \sum_{l=1}^{k+1} (F(u_h(x_{jl}, t))) \Psi_{\xi}(x_{jl}) \omega_l \Delta x,$$

Fully discrete ELDG: SSP RK time discretization

- ▶ Denote $\tilde{U}_h = \int_{\tilde{I}_j(t)} u\psi dx = \int_{I_j} u_h \Psi J d\xi$ with $J = \frac{\partial \tilde{x}(t;(\xi, t^{n+1}))}{\partial \xi}$;
- ▶ Denote the spatial discretization operator as $\mathcal{L}(\tilde{U}_h(t), t)$.

$$\frac{\partial}{\partial t} \tilde{U}_h(t) = \mathcal{L}(\tilde{U}_h(t), t), \text{ with } \tilde{U}_h(t^n) = \tilde{U}_h^n.$$

SSP RK methods:

1. Evaluate $\tilde{U}_h^n = \int_{I_j^*} u(x, t^n) \psi(x, t^n) dx$ at t^n for all test functions Ψ by the **SLDG** scheme.
2. For RK stages $i = 1, \dots, s$, compute

$$\tilde{U}_h^{(i)} = \sum_{l=0}^{i-1} \left[\alpha_{il} \tilde{U}_h^{(l)} + \beta_{il} \Delta t^n \mathcal{L}(\tilde{U}_h^{(l)}, t^n + d_l \Delta t^n) \right].$$

Order	α_{il}	β_{il}	d_l
3	1	1	0
	$\frac{3}{4}$ $\frac{1}{4}$	0 $\frac{1}{4}$	1
	$\frac{1}{3}$ 0 $\frac{2}{3}$	0 0 $\frac{2}{3}$	$\frac{1}{2}$

Allow for a large time step

- ▶ Similar to the time step of DG method, we may use the following time step

$$\Delta t \leq \frac{\Delta x}{(2k + 1) \max |a(x, t) - \alpha(x, t)|}.$$

- ▶ $\alpha(x, t)$ in approximation of $a(x, t)$

$$\max |a(x, t) - \alpha(x, t)| = O(\Delta t) + O(\Delta x^2)$$

⇓

$$\Delta t \sim \Delta x^{\frac{1}{2}},$$

to be verified by the numerical results.

A modified adjoint problem for 2D transport

- ▶ 2D linear transport equation:

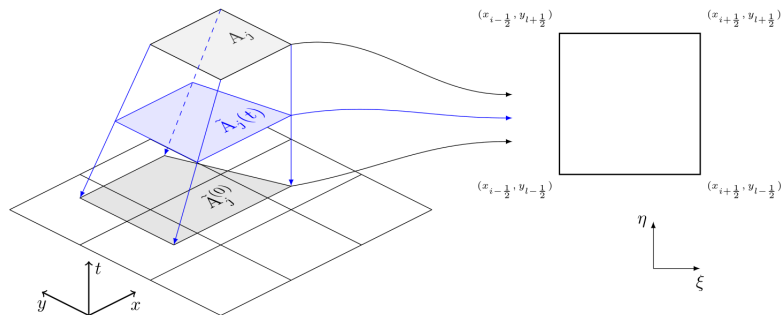
$$u_t + (a(x, y, t)u)_x + (b(x, y, t)u)_y = 0.$$

- ▶ We consider a modified adjoint problem at $\tilde{A}_j(t)$ on the time interval $t \in [t^n, t^{n+1}]$:

$$\psi_t + \alpha(x, y, t)\psi_x + \beta(x, y, t)\psi_y = 0, \quad \psi(x, y, t = t^{n+1}) = \Psi(x, y) \in P^k(A_j),$$

where (α, β) are Q^1 or P^1 polynomials on A_j at t^{n+1} approximating the original velocity field (a, b) .

2D ELDG formulation



$$\frac{d}{dt} \int_{\tilde{A}_j(t)} u \psi dx dy = - \int_{\partial \tilde{A}_j(t)} \psi \hat{\mathbf{F}} \cdot \mathbf{n} dS + \int_{\tilde{A}_j(t)} \mathbf{F} \cdot \nabla \psi dx dy,$$

with

$$\mathbf{F}(u, x, y, t) = \begin{pmatrix} (a(x, y, t) - \alpha(x, y, t))u \\ (b(x, y, t) - \beta(x, y, t))u \end{pmatrix}.$$

2D ELDG formulation on the reference element

► Jacobian, $J(\xi, \eta) = \frac{\partial(\tilde{x}, \tilde{y})}{\partial(\xi, \eta)}(\tau) = \begin{pmatrix} 1 - \frac{\partial\alpha}{\partial\xi}(t^{n+1} - \tau) & \frac{\partial\alpha}{\partial\eta}(t^{n+1} - \tau) \\ -\frac{\partial\beta}{\partial\xi}(t^{n+1} - \tau) & 1 - \frac{\partial\beta}{\partial\eta}(t^{n+1} - \tau) \end{pmatrix}$.

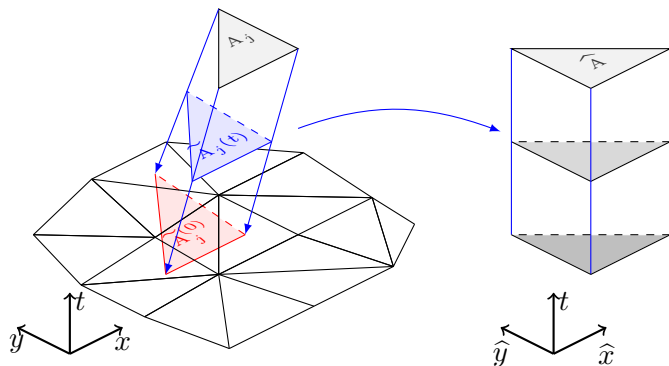
► Mapping formulas:

- $dxdy = \det(J(\xi, \eta))d\xi d\eta$,
- $\nabla_{x,y}\psi(x, y) = J(\xi, \eta)^{-1}\nabla_{\xi,\eta}\Psi(\xi, \eta)$,
- $\mathbf{n}dS = \det(J(\xi, \eta))J(\xi, \eta)^{-T}\check{\mathbf{n}}d\check{S}$.

$$\begin{aligned} & \frac{d}{dt} \int_{A_j} u(\tilde{x}(t, (\xi, \eta, t^{n+1})), \tilde{y}(t, (\xi, \eta, t^{n+1})), t) \Psi(\xi, \eta) \det(J(\xi, \eta)) d\xi d\eta \\ &= - \int_{\partial A_j} \Psi(\xi, \eta) \mathbf{F} \cdot (\det(J(\xi, \eta)) J(\xi, \eta)^{-T} \check{\mathbf{n}}) d\check{S} \\ &+ \int_{A_j} \mathbf{F} \cdot (J(\xi, \eta)^{-1} \nabla_{\xi, \eta} \Psi) \det(J(\xi, \eta)) d\xi d\eta. \end{aligned}$$

Similar to the procedure of 1D ELDG, SSP RK discretization can be applied to the above formulation.

EL RKDG on the unstructured mesh



Summary: EL-RKDG

- ▶ An organic coupling of SL DG and Eulerian RK DG methods
 - ▶ Step 1 (SLDG): L^2 re-projection of solutions on upstream cells.
 - ▶ Step 2 (RKDG): flux differences between original and adjoint problems over the time-dependent dynamic volumes.
- ▶ A unified framework to accommodate both SL and RK DG methods.
 - ▶ RK DG: $\alpha = 0$.
 - ▶ SL DG: $\alpha(x, t)$ follows the exact characteristics.
- ▶ Let Δt_{ELDG} be stability constraint of the ELDG.

$$\Delta t_{ELDG} \in [\Delta t_{RKDG}, \Delta t_{SLDG}]$$

- ▶ High order accuracy, mass conservation, superconvergence, unstructured mesh.

1D transport equation with variable coefficients

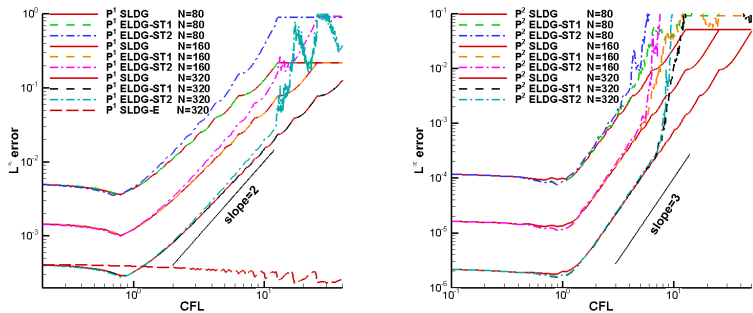
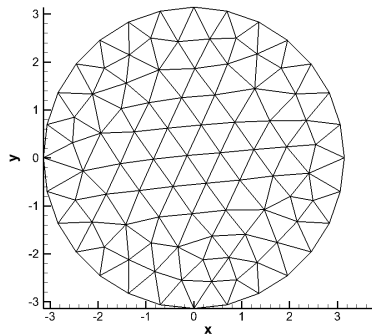


Figure: P^1 SLDG-E means P^1 SLDG scheme which solve the characteristic line exactly. Observations: (1) expected order of convergence in time is observed; (2) Stability bounds for the maximum CFLs of P^2 ELDG using $N = 80, 160, 320$ are observed to be around 3.5, 5, 7 increasing at the ratio of $\sqrt{2} \approx 1.4$, which verifies the time step estimate $\Delta t \sim C\sqrt{\Delta x}$.

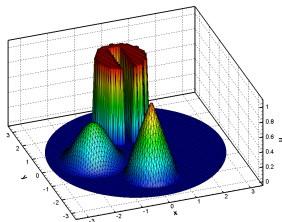
Rigid body rotation

$$u_t - (yu)_x + (xu)_y = 0$$

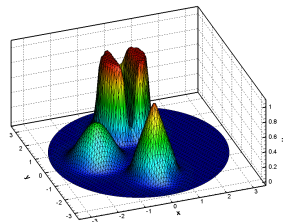
- ▶ A circle domain:
 $(x, y) \in \{(x, y) | x^2 + y^2 \leq \pi^2\}$
- ▶ A sample mesh with the mesh 160 (GMSH).



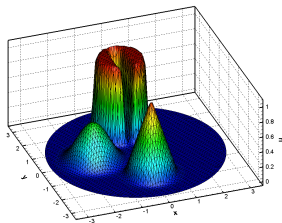
Rigid body rotation: high resolution



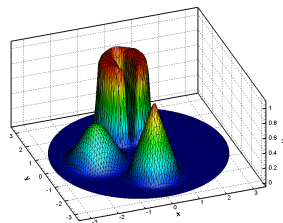
(a) initial state $N = 7432$



(b) P^2 RKDG, $CFL = 0.15$



(c) P^2 SLDG, $CFL = 10.2$



(d) P^2 ELDG, $CFL = 10.2$

Swirling deformation flow: high order spatial and temporal accuracy

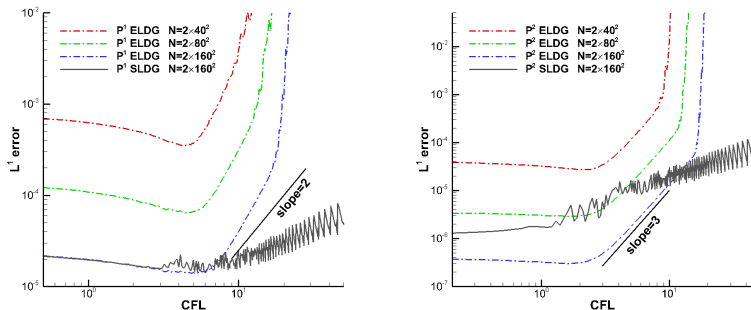
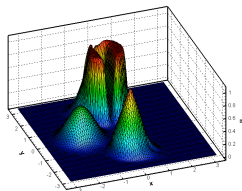
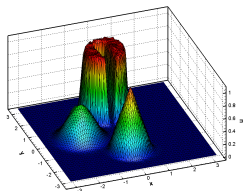


Figure: The swirling deformation flow with the smooth cosine bells with $T = 1.5$. High order spatial and temporal accuracy, large CFL range increase with mesh refinement.

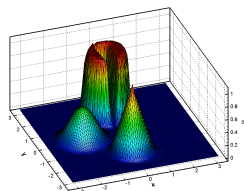
Swirling deformation flow: DG P^2



(a) RKDG, $CFL = 0.15$



(b) SLDG, $CFL = 10.2$



(c) ELDG, $CFL = 10.2$

SLDG-RKEI and ELDG-RKEI methods

- ▶ So far, SLDG and ELDG solvers are proposed for linear transport equations.
- ▶ In order to solve the following **nonlinear** transport problem

$$u_t + \nabla_{\mathbf{x}} \cdot (\mathbf{P}(u; \mathbf{x}, t)u) = 0$$

we apply a high order Runge-Kutta exponential integrator[§], which **decomposes the equation into a set of linearized transport problems.**

For example, a third order SLDG-CF3C03 scheme can be implemented as

$$\begin{aligned}u^{(1)} &= u^n \\u^{(2)} &= SLDG \left(\frac{1}{3} \mathbf{P}(u^{(1)}), \Delta t \right) u^{(1)} \\u^{(3)} &= SLDG \left(\frac{2}{3} \mathbf{P}(u^{(2)}), \Delta t \right) u^{(1)} \\u^{n+1} &= SLDG \left(-\frac{1}{12} \mathbf{P}(u^{(1)}) + \frac{3}{4} \mathbf{P}(u^{(3)}), \Delta t \right) u^{(2)}.\end{aligned}$$

[§]Celledoni, et al., FGCS ,2003

The guiding center Vlasov model

The guiding center model describes a highly magnetized plasma in the transverse plane of a tokamak. It reads

$$\rho_t + \nabla \cdot (\mathbf{E}^\perp \rho) = 0,$$

$$-\Delta \Phi = \rho, \quad \mathbf{E}^\perp = (-\Phi_y, \Phi_x)$$

where ρ is the charge density of the plasma and $\mathbf{E} = (E_1, E_2)$ determined by $\mathbf{E} = -\nabla \Phi$ is the electric field.

Guiding center Vlasov: high order spatial accuracy

Table: Guiding center Vlasov on the domain $[0, 2\pi] \times [0, 2\pi]$ with the initial condition $\omega(x, y, 0) = -2 \sin(x) \sin(y)$. $T = 1$. $CFL = 1$. The temporal scheme CF3C03 is used.

Mesh	L^1 error	Order	L^1 error	Order
	P^1 SLDG		P^1 ELDG	
20^2	1.39E-02	–	9.59E-03	–
40^2	3.66E-03	1.93	2.35E-03	2.03
60^2	1.65E-03	1.97	1.02E-03	2.06
80^2	9.37E-04	1.96	5.78E-04	1.97
100^2	6.01E-04	1.99	3.69E-04	2.00
	P^2 SLDG-QC		P^2 ELDG	
20^2	2.13E-03	–	1.54E-03	–
40^2	2.73E-04	2.97	1.79E-04	3.10
60^2	8.11E-05	2.99	5.21E-05	3.05
80^2	3.48E-05	2.94	2.10E-05	3.16
100^2	1.77E-05	3.02	1.07E-05	3.04

Guiding center Vlasov: high order temporal accuracy & huge time step!

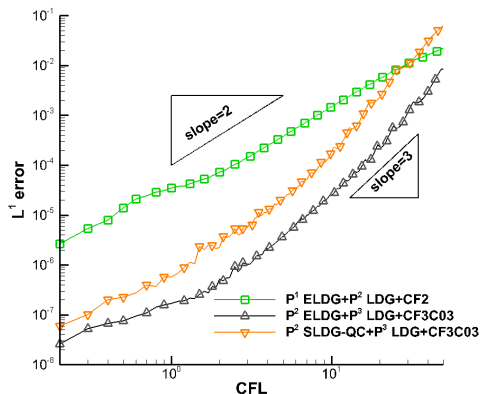


Figure: The Kelvin-Helmholtz instability problem at $T = 5$. The mesh of 120×120 cells is used. The reference solution from the corresponding scheme with $CFL = 0.1$.

SLDG-QC with adaptive time stepping algorithm for guiding center Vlasov

3D plot of solutions of third order SLDG-QC-RKEI method with the adaptive time-stepping algorithm based on the area invariant, $\max_j \left| \frac{\text{area}(A_j^*) - \text{area}(A_j)}{\text{area}(A_j)} \right|$. The mesh is 100×100 .

Summary and future work

We propose an ELDG method, which avoids to construct a quadratic-curved quadrilaterals and still enjoys

- ▶ high order DG spatial discretization, high order temporal discretization, **large time stepping size**, mass conservation, resolution of filamentations, superconvergence of long time integration.
- ▶ SLDG + ALE + characteristics tracking/approximation

Further development ELDG:

- ▶ linear system such as the wave equation
- ▶ handling diffusion and stiff source terms with asymptotic preserving properties
- ▶ positivity preserving ELDG
- ▶ nonlinear hyperbolic conservation laws, such as Burgers', shallow water, Euler and Navier-Stokes systems.

References

- ▶ An Eulerian-Lagrangian discontinuous Galerkin method for transport problems and its application to nonlinear dynamics, w/ Cai and Yang, arXiv, 2002.02930.
- ▶ High Order Semi-Lagrangian Discontinuous Galerkin Method Coupled with Runge-Kutta Exponential Integrators for Nonlinear Transport Problems, w/ Cai and Boscarino, JCP, 2021.
- ▶ Comparison of semi-Lagrangian discontinuous Galerkin schemes for linear and nonlinear transport simulations, with Cai and Guo, CAMC, accepted.
- ▶ A semi-Lagrangian discontinuous Galerkin (DG) - local DG method for solving convection-diffusion-reaction equations, w/ Ding, Cai, Guo, Journal of Computational Physics, JCP, 2020.
- ▶ A high order semi-Lagrangian discontinuous Galerkin method for the two-dimensional incompressible Euler equations and the guiding center Vlasov model without operator splitting, with Cai and Guo, JSC, 2019.
- ▶ A high order semi-Lagrangian discontinuous Galerkin method for Vlasov-Poisson simulations without operator splitting, with Cai and Guo, JCP, 2018.
- ▶ A high order conservative semi-Lagrangian discontinuous Galerkin method for two-dimensional transport simulations, with Cai and Guo, JSC, 2017.